Effects of doxorubicin and gemcitabine on the induction of apoptosis in breast cancer cells

RUI-RUI ZHENG, WEI HU, CHENG-GUANG SUI, NAN MA and YOU-HONG JIANG

Cancer Research Institute, The First Affiliated Hospital, China Medical University, Shenyang, Liaoning 110001, P.R. China

Received June 25, 2014; Accepted September 3, 2014

DOI: 10.3892/or.2014.3513

Abstract. Breast cancer is the most frequently diagnosed cancer and the leading cause of cancer-related mortality in females worldwide. The efficacy of chemotherapeutic drugs on breast cancer is hindered by many factors, including that cancer stem-like side population (SP) cells may contribute to tumorigenesis and resistance to chemotherapy. Doxorubicin and gemcitabine are two of the most effective and widely used chemotherapeutic agents for the treatment of various human malignancies. To the best of our knowledge, the effects of doxorubicin and gemcitabine on breast cancer SP cells are poorly understood. In the present study, we examined the potential roles of doxorubicin and gemcitabine in breast cancer main population (MP) and SP cells, and the mechanisms of doxorubicin and gemcitabine. The results showed that doxorubicin and gemcitabine decreasede proliferation, and increased apoptosis in the MCF7 MP and SP cells *in vitro*. Furthermore, doxorubicin and gemcitabine inhibited tumor growth and improved the survival rate of mice *in vivo*. Additionally, the mechanisms of doxorubicin and gemcitabine in MCF7 MP and SP cells were determined.

Introduction

Breast cancer is the most frequently diagnosed cancer and the leading cause of cancer-related mortality in females worldwide (1). While significant treatment advances have been made, all patients face the risk of disease recurrence, which is the main cause of death from breast cancer (2). In recent years, studies on cancer development and recurrence have been influenced by side population (SP) cells (3). SP cells are a small subpopulation of cells with enriched stem cell activity (4). Dye exclusion is a valuable technique successful in isolating and identifying SP cells, based on stem cells possessing a high ability to exclude fluorescent DNA-binding dye, Hoechst 33342 (5-7).

Correspondence to: Professor You-Hong Jiang, Cancer Research Institute, The First Affiliated Hospital, China Medical University, 155 North Nanjing Road, Shenyang, Liaoning 110001, P.R. China
E-mail: jyouhong@126.com

Key words: breast cancer, side population, doxorubicin, gemcitabine, apoptosis

Gemcitabine [2',2'-difluorodeoxycytidine (dFdC)] is a pyrimidine nucleoside analogue of deoxycytidine commonly used in non-small-cell lung cancer (NSCLC) and breast cancer (8,9). Gemcitabine is phosphorylated by deoxycytidine kinases, which then incorporate into DNA to inhibit synthesis and cell proliferation, while promoting apoptosis in cancer cells (10). Doxorubicin is one of the most effective and widely used chemotherapeutic agents for the treatment of various human malignancies (11,12).

To the best of our knowledge, the effects of doxorubicin and gemcitabine on breast cancer cells are poorly understood. The present study addressed, for the first time, the potential killing roles of doxorubicin and gemcitabine in breast cancer SP and main population (MP) cells, as well as the mechanisms of doxorubicin and gemcitabine. This finding may be useful in improving the clinical effectiveness of biotherapy for the treatment of malignant tumors.

Materials and methods

Cell culture. MCF7 cells were purchased from the American Type Culture Collection (ATCC; Rockville, MD, USA) and maintained in RPMI-1640 containing 10% heat-inactivated fetal bovine serum (FBS) and 1% penicillin-streptomycin. Cells were maintained in a humidified cell incubator with 5% CO_2 at 37˚C.

SP cell analysis. MCF7 cells were suspended at $1x10^6$ cells/ml and then incubated at 37˚C for 60 min with 5 μg/ml Hoechst 33342 (Sigma Chemicals, St. Louis, MO, USA). The control cells were cultured in the presence of 500 μM verapamil (Sigma). Analysis and sorting of the SP cells was performed using a FACS VantageSE cytometer (Becton-Dickinson, San Jose, CA, USA). Hoechst 33342 was excited using a UV laser at 350 nm and fluorescence emission was measured at 402-446 and 640 nm for Hoechst blue and red, respectively.

RT-PCR. Total RNA was isolated from MP and SP cells using an RNeasy Mini kit (Biomed, Beijing, China). cDNA was reverse transcribed with 1 μg of total RNA using a Takara Reverse Transcription kit (Takara, Dalian, China) and was amplified using the following primers: *CD133*: 5'-ACCGAC TGAGACCCAACATC-3' (sense), and 5'-GGTGCTGTTCAT GTTCTCCA-3'(antisense)and*ABCG2*:5'-AGCTGCAAGGAA AGATCCAA-3' (sense), and 5'-TCCAGACACACCACG

GATAA-3' (antisense). *GAPDH* primers were: 5'-AGAAGGC TGGGGCTCATTTG-3' (sense), and 5'-AGGGGCCATCCA CAGTCTTC-3' (antisense), and used as an internal control. The PCR products were electrophoresed on a 1.5% agarose gel, and visualized by ethidium bromide staining under a UV imaging system (UVP, LLC, Upland, CA, USA).

Immunofluorescence. Cells were fixed with 4% paraformaldehyde for 15-20 min, washed twice in phosphate-buffered saline (PBS) at room temperature for 5 min and permeabilized in PBS containing 2% Triton X-100 for 30 min. Non-specific binding sites were blocked with 3% bovine serum albumin (BSA) in PBS for 1 h. The primary monoclonal antibody CD133 or ABCG2, diluted in 3% BSA/PBS, was applied overnight at 4˚C. The cells were washed twice with PBS and then exposed to the secondary antibody diluted at 1:100 in 3% BSA/PBS for 1 h. For every coverslip, the cells were observed and photographed in 5 random fields using an Olympus CX71 fluorescence microscope (Olympus, Tokyo, Japan).

Sphere assay. The SP and MP cells were plated at a density of $6x10^4$ cells/well in 6-well, ultra-low attachment plates under serum-free, sphere-specific conditions described by Gibbs *et al* (13). Fresh aliquots of epidermal growth factor (EGF) and basic fibroblast growth factor (bFGF) were added each day. After culture for 7 days, the spheres were visible under a fluorescence microscope, as described above.

Drug and treatment. Doxorubicin (D1515) and gemcitabine (Y0000676) were purchased from Sigma. MCF7 MP cells were designed as group 1 (control group, no treatment with drugs); group 2 (1 μg/ml, doxorubicin-treated MP cells); group 3 (1 μg/ml, gemcitabine-treated MP cells); MCF-7 SP cells were designed as group 4 (control group, no treatment with drugs); group 5 (1 μg/ml, doxorubicin-treated SP cells); and group 6 (1 μg/ml, gemcitabine-treated SP cells).

3-[4,5-Dimethylthiazol-2-yl]-2,5-diphenyltetrazolium bromide (MTT) assay. The proliferation rate of the treated and control cells was measured by MTT assay. Briefly, for the MTT assay, treated or control cells were plated at a density of $1x10^3$/well in 96-well plates and incubated for 48 h under complete culture medium containing 0.5 mg/ml MTT (Sigma). Four hours later, the medium was replaced with 100 μl dimethyl sulfoxide (DMSO) (Sigma) and vortexed for 10 min to dissolve the crystals. Absorbance optical density (OD) of each well was determined at a wavelength of 490 nm with subtraction of baseline reading.

Apoptosis assay. For the apoptosis assay, equal numbers of cells were seeded in 6-cm plates. Following the manufacturer's instructions (Apoptosis Detection kit; KeyGen, Nanjing, China), the cells were trypsinized, washed twice with cold PBS, and resuspended in 200 μl binding buffer. Annexin V-FITC was added to a final concentration of 0.5 μg/ml. Samples were incubated at room temperature in the dark. After 20 min, 300 μl binding buffer containing 0.5 μg/ml PI was added and samples were immediately analyzed on a FACSCalibur flow cytometer (Becton-Dickinson Medical Devices, Shanghai, China). Cells in the stages of early apoptosis were defined as $FITC^+/PI^-$ cells.

Determination of mitochondrial membrane potential (MMP). MMP was analyzed using the fluorescent dye 5,5',6,6'-tetrachloro-1,1',3,3'-tetraethylbenzimidazolycarbocyanine iodide (JC-1) following the manufacturer's instructions (KeyGen). Briefly, the cells were plated in 6-well culture plates. After treatment for 24 h, the cells were washed twice with PBS, harvested and incubated with 20 nM JC-1 for 30 min in the dark. MMP was subsequently analyzed using the FACSCalibur machine, as described above.

Quantification of cellular reactive oxygen species (ROS). Cells ($5x10^5$) were cultured in 12-well tissue culture plates overnight, and then co-treated with drugs and 2',7'-dichlorofluorescein diacetate, a ROS-sensitive dye (KeyGen). After drug treatment, the cells were harvested and suspended in PBS. Relative fluorescence intensities of cells were quantified using the FACSCalibur machine, as described above.

Adhesion assay. The adhesion ability of cancer cells was examined using the adhesion assay. Six-well plates were coated with collagen I (10 μg/ml), fibronectin (10 μg/ml) or growth factor-reduced Matrigel (10 μg/ml) (BD Biosciences), with 1% BSA as the control. The cells were harvested with trypsin-EDTA and resuspended in serum-free medium. The cells were allowed to attach at 37˚C for 1 h. Unbound cells were removed by washing twice with PBS. Attached cells were fixed in 4% paraformaldehyde and counted. Cell counts were obtained by averaging the cell numbers from five wells. The percentage of cells adhering was calculated as: % bindings = (OD of treated surface-only ECM component)/OD of total surface x 100.

Cell invasion assay. For the invasive assay, the cells were resuspended in serum-free RPMI-1640 and seeded in the control-membrane insert on the top portion of the Matrigel-coated chamber (BD Biosciences). The lower compartment of the chamber contained 10% FBS as a chemoattractant. After incubation for 24 h, the cells on the membrane were scrubbed, washed with PBS and fixed in 100% methanol and stained with Giemsa dye (KeyGen).

Transplantation experiment. Sorted SP and MP cells were collected, and the cells were resuspended in HBSS. Cell suspension was then mixed with Matrigel (1:1). This cell-Matrigel suspension was then subcutaneously injected into 4-week-old BALB/C-nu/nu nude mice (male) obtained from the Shanghai Laboratory Animal Center of China under anesthesia. Groups of mice were inoculated with SP cells at $1x10^5$ or MP cells at $1x10^7$. The mice were examined once every 5 days and tumor growth was evaluated by measuring the length and width of the tumor. The mice were sacrificed and tumor masses were removed and fixed in 10% neutral-buffered formalin solution for histological preparations.

Immunohistochemistry (IHC). Sections (4 μm) were baked at 65˚C for 30 min, and then deparaffinized with xylene and rehydrated. The sections were submerged into EDTA (pH=8.0), autoclaved for antigen retrieval, and treated with 3% hydrogen peroxide, followed by incubation with 1% FBS. The primary antibody was added and incubated overnight at 4˚C. Horseradish peroxidase (HRP)-labeled secondary antibody in

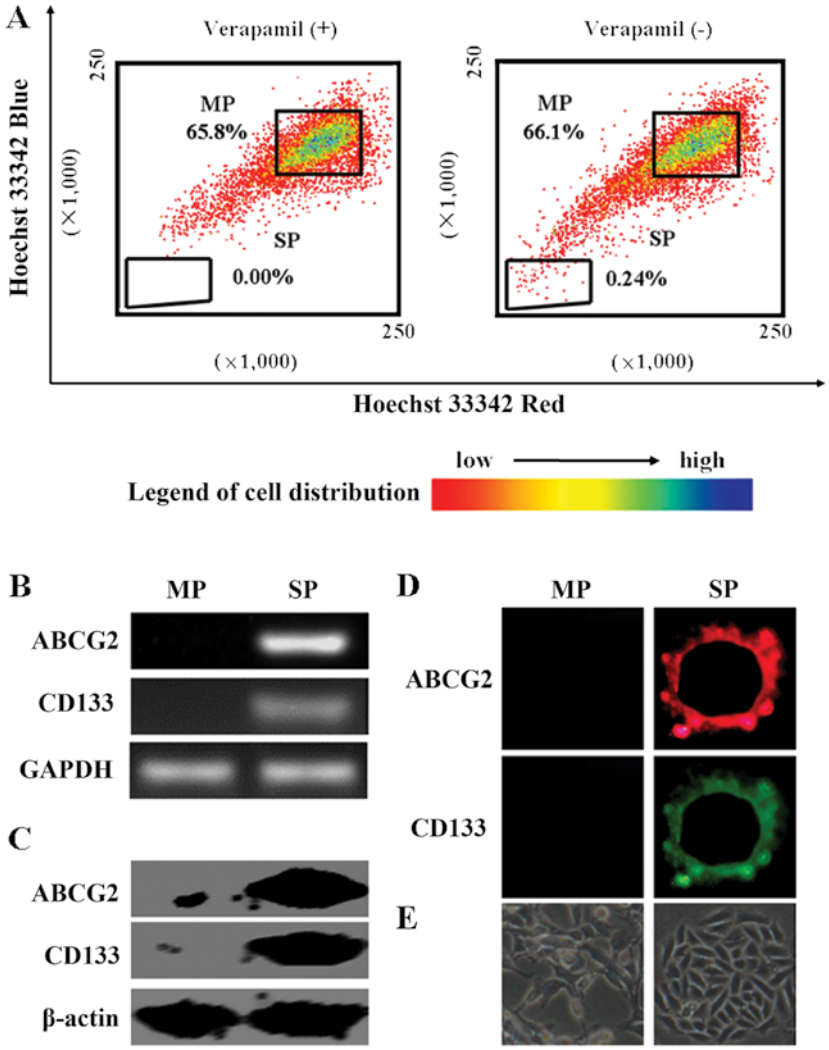

Figure 1. Identification of side population (SP) and main population (MP) cells in MCF7 cell lines. (A) MCF7 cells were isolated by using FACSVantage SE. (B) The mRNA levels of *ABCG2* and *CD133* were determined by RT-PCR. (C) Cellular protein was isolated from MP and SP cells, and the expression of ABCG2 and CD133 proteins was determined by western blotting. (D) The expression and location of ABCG2 and CD133 proteins were also examined by immunofluorescence. (E) Representative images of a sphere cluster formed by SP cells after 7 days and no sphere clusters were formed by MP cells.

the MaxVision™ HRP-Polymer anti-Mouse/Rabbit IHC kit (KIT-5930; Maixin Biology, Fuzhou, China) was applied and incubated for 30 min, followed by 5 min incubation with DAB, provided in the kit for color development. The sections were then counterstained with hematoxylin and mounted. The results were visualized and photographed under a light microscope.

PHYRE database was used to generate predicted structural models. The protein sequence of ABCG2 was obtained from the PubMed (http://www.ncbi.nlm.nih.gov/protein/AAG52982.1) and submitted to the Protein Homology/analogY Recognition Engine (PHYRE; version 2). Based on the homology sequence in the PHYRE server, the three-dimensional structure of the ABCG2 protein was predicted.

Preparation of proteins and ligand structures for docking. We applied this approach to the predicted structural model of ABCG2. The molecular structures of doxorubicin (CID 31703) and gemcitabine (CID 60750) were downloaded from PubChem Compound (http://www.ncbi.nlm.nih.gov/pccompound). Data were imported into the modeling software SYBYL-X 1.3 (Tripos International, St. Louis, MO, USA). Non-protein components such as water molecules, metal ions and lipids were deleted, and hydrogen atoms were added to the protein structures. The interaction of doxorubicin or gemcitabine and ABCG2 was analyzed by SYBYL-X 1.3.

SDS-PAGE and immunoblotting. Proteins (30 μg/lane) were separated by 10% SDS-polyacrylamide gel electrophoresis and transferred to PVDF membranes (Millipore Corporation, Billerica, MA, USA). Western blotting was performed using primary antibodies: anti-ABCG2 (4477; 1:200) was purchased from Cell Signaling Technology (Beverly, MA, USA), and anti-CD133 (MAB4310; 1:200) was purchased from Millipore Corporation. Anti-Bax (sc-7480; 1:500), anti-Bcl-xL (sc-8392; 1:500), anti-Bcl-2 (sc-783; 1:500), anti-phospho-Bcl-2 (Ser 87) (sc-16323; 1:500) and β-actin (sc-47778; 1:1,000) were purchased from Santa Cruz Biotechnology, Inc. (Santa Cruz, CA, USA). Incubation with antibodies was performed in 1.5% BSA in TBS, 0.1% Tween. Detection of the immune complexes was performed with the ECL Plus Western Blotting Detection System (Amersham Biosciences, Piscataway, NJ, USA).

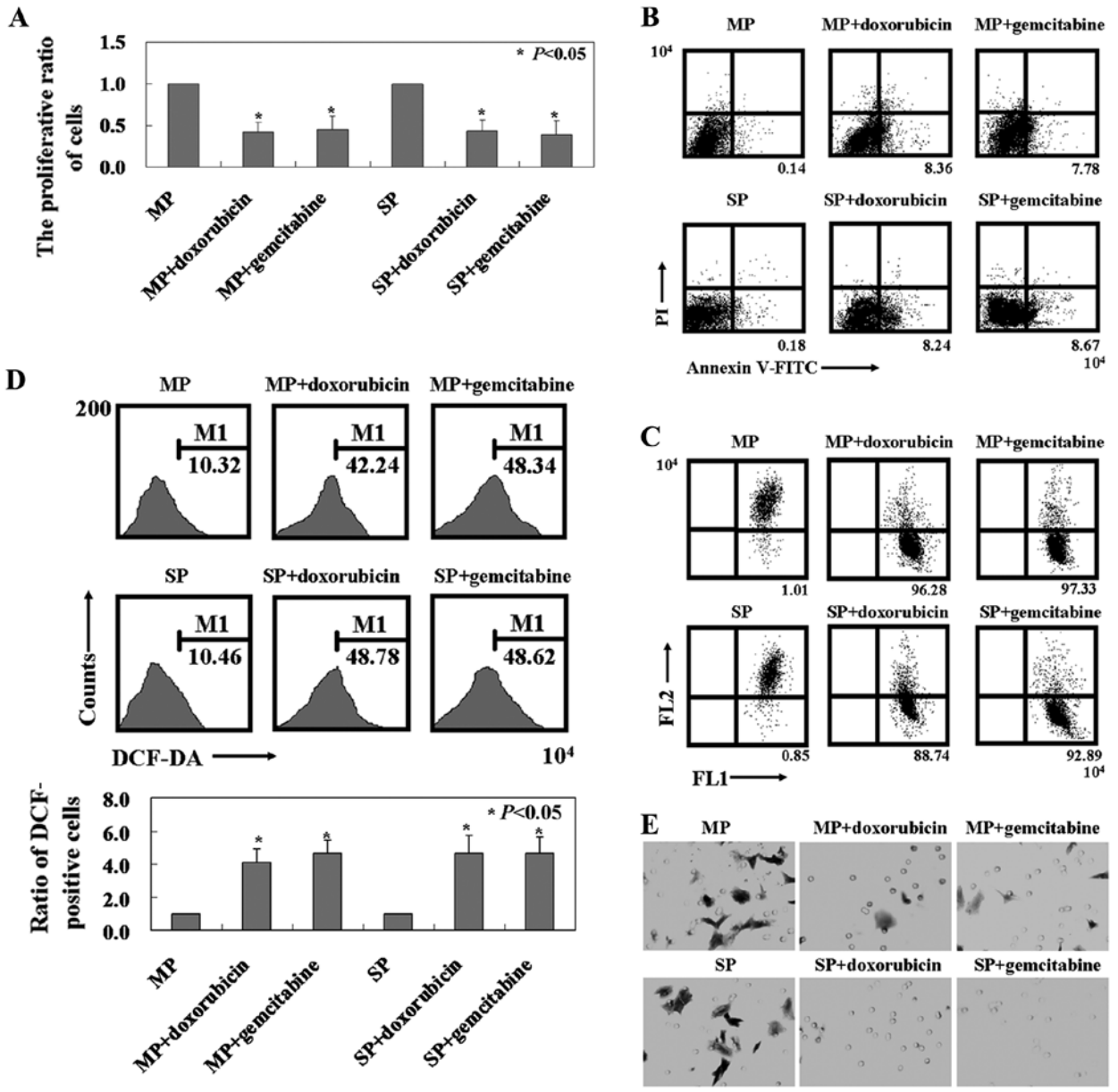

Figure 2. Antitumor activity of gemcitabine or doxorubicin detected in MCF7 MP and SP cells. (A) Growth curves of MCF7 MP and SP cells treated with gemcitabine or doxorubicin. (B) The proportion of early apoptotic cells ($FITC^+/PI^-$ cells) detected by flow cytometry. (C) Mitochondrial membrane potential was analyzed by flow cytometry. (D) The DCF-positive cells (ROS production) were detected with an FL1 signal detector (525 nm) using a FACSCalibur machine. (E) Transwell assays were performed. Cells that migrated to the bottom side of the membrane were stained and counted. MP, main population; SP, side population; ROS, reactive oxygen species.

Statistical analysis. Data are presented as means ± SD. The statistical significance of differences was determined by Student's two-tailed t-test in two groups and one-way ANOVA in multiple groups. Kaplan-Meier survival plots were generated and comparisons between survival curves were made with the log-rank statistic. P<0.05 was considered to indicate a statistically significant result. Data were analyzed with GraphPad Prism 5 (San Diego, CA, USA).

Results

SP fraction in MCF7 cells. The SP cell fraction comprised 0.24% of the total MCF7 cells, and this population disappeared following treatment with the selective ABCG2 transporter inhibitor, verapamil (Fig. 1A). In addition, we showed that CSC-specific markers, ABCG2 and CD133 mRNA, and proteins were significantly increased in the SP cells when compared with those in MP cells (Fig. 1B and C). Immunofluorescence results showed that ABCG2 and CD133 were localized in the membrane of the SP cells (Fig. 1D). After 7 days of culture, sphere clusters were clearly observed in the SP cultures, while MP cells did not form spheres (Fig. 1E).

Effects of doxorubicin or gemcitabine on the proliferation, apoptosis, MMP and mobility of MCF7 cells. As shown in Fig. 2A, doxorubicin and gemcitabine decreased the cell viability of MCF7 SP and MP cells (P<0.05). In addition, doxorubicin or gemcitabine-induced apoptosis was detected in the

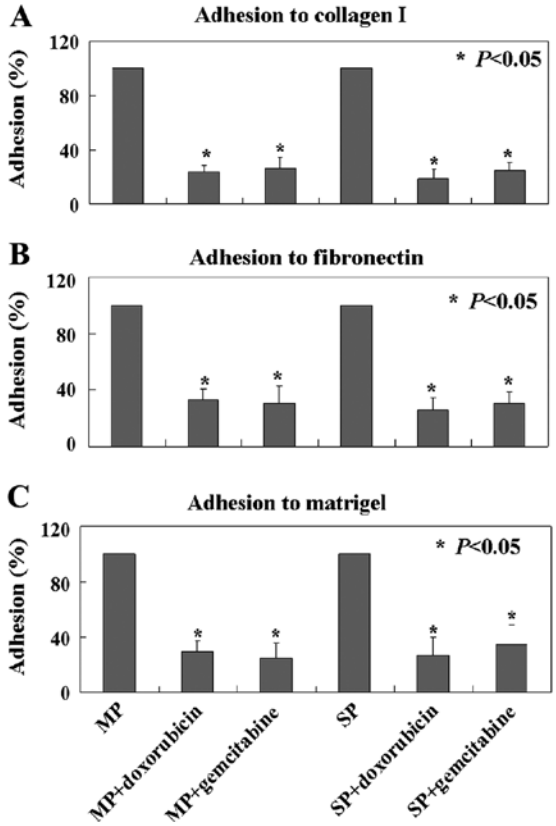

Figure 3. MCF7 MP and SP cells were allowed to adhere for 45 min to type I (A) collagen, (B) fibronectin or (C) Matrigel in the presence of gemcitabine or doxorubicin. MP, main population; SP, side population.

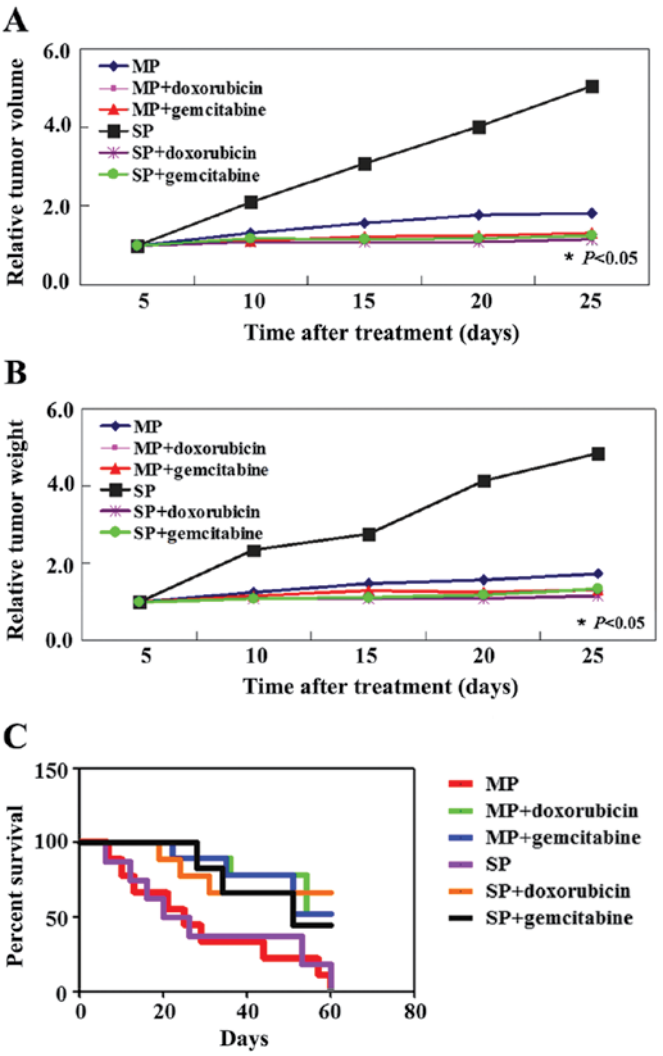

Figure 4. Doxorubicin or gemcitabine suppresses MCF7 MP and SP cells tumor growth *in vivo*. (A and B) After tumors reached a diameter of 3-5 mm, the tumors were directly injected with doxorubicin or gemcitabine. Tumor volume and weight were measured for each tumor group on days 5, 10, 15, 20 and 25. (C) Kaplan-Meier survival curves of the groups were assessed as described in Materials and methods. MP, main population; SP, side population

SP and MP cells by Annexin V/PI double staining (Fig. 2B). Changes in MMP were detected in MCF7 MP and SP cells after doxorubicin or gemcitabine treatment by using flow cytometry (Fig. 2C). Furthermore, the level of ROS content was significantly increased in MCF7 MP and SP cells after doxorubicin or gemcitabine treatment compared to untreated MP and SP cells using the fluorescent dye DCF-DA (P<0.05, Fig. 2D). Based on these results, we hypothesized that doxorubicin- or gemcitabine-induced apoptosis in MCF7 MP and SP cells was associated with the mitochondrial apoptotic signaling pathway. Since breast cancer has a high rate of metastasis, we determined whether there were any mobility changes in MCF7 MP and SP cells after doxorubicin or gemcitabine treatment using the Transwell assay. We found that significantly less MCF7 MP and SP cells with doxorubicin or gemcitabine treatment migrated to the lower membrane compared to control cells (Fig. 2E). In ECM-mediated adhesion, MCF7 MP and SP cells with doxorubicin or gemcitabine treatment showed significantly less adhesion to type I collagen, fibronectin and Matrigel compared to the untreated MCF7 MP and SP cells (Fig. 3).

Doxorubicin or gemcitabine inhibits tumor growth and improves survival rate of mice in vivo. We determined whether doxorubicin or gemcitabine exhibits antitumor properties in established xenograft tumor models. As shown in Fig. 4A and B, the tumor volume of doxorubicin or gemcitabine-treated MP mice was less than that of the untreated MP mice (P<0.05). Tumor weight was significantly decreased in the doxorubicin or gemcitabine-treated MP group compared to the untreated group by 20 days after treatment (P<0.05). Similar results were observed in the SP group (P<0.05, Fig. 4A and B). We also found that doxorubicin or gemcitabine-treated mice had an improved survival rate compared to the untreated mice (P<0.05, Fig. 4C). In the untreated groups, the mice needed to be sacrificed due to tumor burden or organ failure beginning 5 days after treatment. However, mice in the doxorubicin- or gemcitabine-treated group did not need to be sacrificed until 20 days after treatment. The survival rate of the doxorubicin or gemcitabine-treated group was 50% when compared to the control groups.

Doxorubicin or gemcitabine binds to ABCG2 and activates the mitochondrial apoptotic signaling pathway in MCF MP and SP cells. To examine the possible mechanisms whereby doxorubicin or gemcitabine could play roles in SP and MP cells, we applied the modeling software SYBYL-X 1.3 and

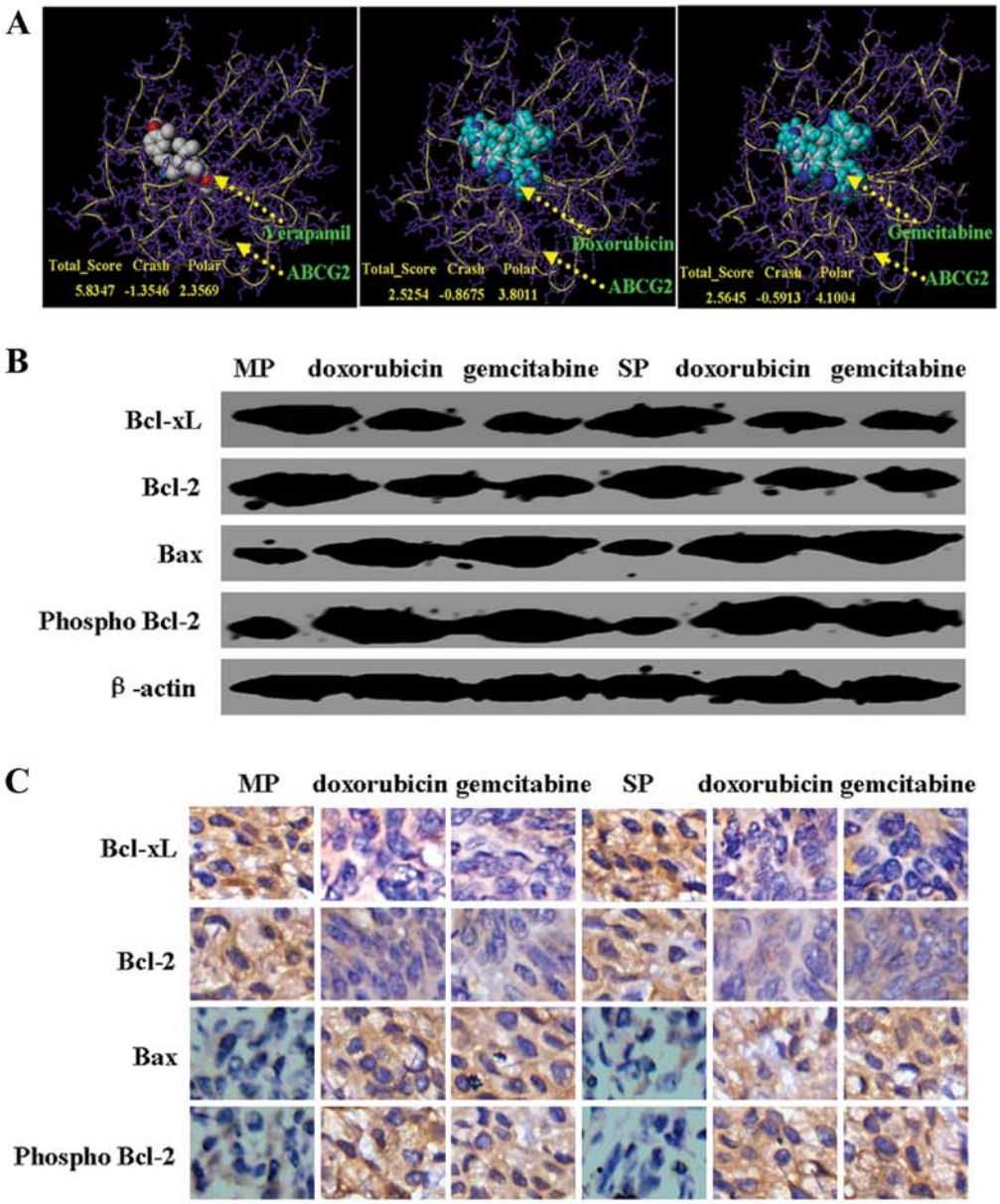

Figure 5. Effects of doxorubicin or gemcitabine on the mitochondrial apoptotic pathway. (A) Position of interaction sites in a model of verapamil, doxorubicin or gemcitabine bound to the ABCG2 protein. (B) Levels of Bcl-xL, Bcl-2, Bax and phosphorylated forms of Bcl-2 were detected in western blot analyses of cell lysates. β-actin was used as an internal control. (C) Levels of Bcl-xL, Bcl-2, Bax and phosphorylated forms of Bcl-2 were detected by using IHC. p-Bcl-2, phospho Bcl-2; IHC, immunohistochemistry.

found that doxorubicin or gemcitabine was able to dock into ABCG2 (Fig. 5A). Interesting, the docking position of doxorubicin or gemcitabine in ABCG2 was similar to verapamil (Fig. 5A). In order to identify the mechanism of action of doxorubicin or gemcitabine in MCF7 MP and SP cells, we detected the protein expression of Bax, Bcl-2, p-Bcl-2 and Bcl-xL by western blot analysis. We found a decrease in Bcl-2 and Bcl-xL protein as well as an increase in p-Bcl-2 and Bax protein levels in MCF7 MP and SP cells with doxorubicin or gemcitabine treatment (Fig. 5B). Furthermore, we confirmed our results *in vivo* by using IHC (Fig. 5C).

Discussion

ABCG2 is one of the human ABC transporters that are involved in multidrug resistance (MDR) in cancer chemotherapy (14,15). The *ABCG2* gene, located on chromosome 4, is >66 kb and contains 16 exons and 15 introns (16). ABCG2 is a 655 amino acid, 72-kDa protein with a single ABC signature domain within the nucleotide-binding domain and six transmembrane domains (17). Previous studies of the role of drug efflux in resistance to doxorubicin or gemcitabine have yielded controversial results. Zhou *et al* (18) suggested that the expression of ABCB1 and ABCG2 (BCRP) transporters may contribute to gemcitabine resistance and tumor relapse. However, Bergman *et al* (19) reported that the expression of ABCB1 and ABCC1 (MRP1) enhances gemcitabine sensitivity. Doxorubicin or gemcitabine have been shown to possess a broad antitumor activity against breast, lung, ovarian, bladder and pancreatic cancer (10-12). In the present study, we found that doxorubicin or gemcitabine inhibited MCF7 MP and SP cells. We hypothesized that the high intracellular accumulation

of doxorubicin or gemcitabine in MCF7 MP and SP cells was a consequence of the decreased activity of ABCG2. Notably, we found that the docking position of doxorubicin or gemcitabine in ABCG2 was similar to that of verapamil. Verapamil is a non-selective pharmacological inhibitor of ABC transporter family members (20). Future studies should be conducted to determine the roles of doxorubicin or gemcitabine in ABCG2.

Furthermore, we found that doxorubicin- or gemcitabine-induced apoptosis in MP and SP cells were associated with loss of mitochondrial membrane potential (MMP). The disruption of MMP has been reported to be affected by reactive oxygen species (ROS) (21). Consistent with recent studies (22,23), in the present study, we found that ROS is significantly increased in MP and SP cells with doxorubicin or gemcitabine treatment. Bcl-2 and Bcl-xL are two anti-apoptotic proteins and Bax is a pro-apoptotic protein in the mitochondrial apoptotic pathway (22-24). In concordance with the earlier findings, we observed reductions in the expression of Bcl-2 and Bcl-xL in cells treated with doxorubicin or gemcitabine. Consistent with the results by Xia *et al* (22), we also found that p-Bcl-2, an inactivated form of Bcl-2, was significantly increased.

In summary, doxorubicin and gemcitabine decreased the cell viability, induced apoptosis and mitochondrial damage in MCF7 SP and MP cells. Consequently, the mitochondrial apoptotic pathway was activated. Therefore, the present study has expanded our understanding of the role of doxorubicin and gemcitabine in MCF7 SP and MP cells. However, whether the high intracellular accumulation of doxorubicin or gemcitabine in MCF7 MP and SP cells was a consequence of the decreased activity of ABCG2 remains unclear.

Acknowledgements

We would like to thank Miss Ying Zhang for her valuable comments and excellent technical assistance.

References

1. Jemal A, Bray F, Center MM, *et al*: Global cancer statistics. CA Cancer J Clin 61: 69-90, 2011.
2. Glück S and Gorouhi F: Clinical and economic benefits of aromatase inhibitor therapy in early-stage breast cancer. Am J Health Syst Pharm 68: 1699-1706, 2011.
3. Noto A, Raffa S, De Vitis C, *et al*: Stearoyl-CoA desaturase-1 is a key factor for lung cancer-initiating cells. Cell Death Dis 4: e947, 2013.
4. Bonnet D and Dick JE: Human acute myeloid leukemia is organized as a hierarchy that originates from a primitive hematopoietic cell. Nat Med 3: 730-737, 1997.
5. Xia P, Gou WF, Zhao S and Zheng HC: Crizotinib may be used in Lewis lung carcinoma: A novel use for crizotinib. Oncol Rep 30: 139-148, 2013.
6. Ho MM, Ng AV, Lam S, Hung JY: Side population in human lung cancer cell lines and tumors is enriched with stem-like cancer cells. Cancer Res 67: 4827-4833, 2007.
7. Haraguchi N, Utsunomiya T, Inoue H, *et al*: Characterization of a side population of cancer cells from human gastrointestinal system. Stem Cells 24: 506-513, 2006.
8. Schiller JH, Harrington D, Belani CP, *et al*: Comparison of four chemotherapy regimens for advanced non-small-cell lung cancer. N Engl J Med 346: 92-98, 2002.
9. Spielmann M, Llombart-Cussac A, Kalla S, *et al*: Single-agent gemcitabine is active in previously treated breast cancer. Oncology 60: 303-307, 2001.
10. Plunkett W, Huang P, Xu YZ, *et al*: Gemcitabine: metabolism, mechanisms of action, and self-potentiation. Semin Oncol 22 (Suppl 11): S3-S10, 1995.
11. Chatterjee K, Zhang J, Honbo N and Karliner JS: Doxorubicin cardiomyopathy. Cardiology 115: 155-162, 2010.
12. Takemura G and Fujiwara H: Doxorubicin-induced cardiomyopathy from the cardiotoxic mechanisms to management. Prog Cardiovasc Dis 49: 330-352, 2007.
13. Gibbs CP, Kukekov VG, Reith JD, *et al*: Stem-like cells in bone sarcomas: implications for tumorigenesis. Neoplasia 7: 967-976, 2005.
14. Xu J, Peng H and Zhang JT: Human multidrug transporter ABCG2, a target for sensitizing drug resistance in cancer chemotherapy. Curr Med Chem 14: 689-701, 2007.
15. Zhang JT: Biochemistry and pharmacology of the human multidrug resistance gene product, ABCG2. Zhong Nan Da Xue Xue Bao Yi Xue Ban 32: 531-541, 2007.
16. Kanzaki A, Toi M, Neamati N, *et al*: Copper-transporting P-type adenosine triphosphatase (ATP7B) is expressed in human breast carcinoma. Jpn J Cancer Res 93: 70-77, 2002.
17. Robey RW, Ierano C, Zhan Z and Bates SE: The challenge of exploiting ABCG2 in the clinic. Curr Pharm Biotechnol 12: 595-608, 2011.
18. Zhou J, Wang CY, Liu T, *et al*: Persistence of side population cells with high drug efflux capacity in pancreatic cancer. World J Gastroenterol 14: 925-930, 2008.
19. Bergman AM, Pinedo HM, Talianidis I, *et al*: Increased sensitivity to gemcitabine of P-glycoprotein and multidrug resistance-associated protein-overexpressing human cancer cell lines. Br J Cancer 88: 1963-1970, 2003.
20. Nobili S, Landini I, Giglioni B and Mini E: Pharmacological strategies for overcoming multidrug resistance. Curr Drug Targets 7: 861-879, 2006.
21. Liu ZH and Lenardo MJ: Reactive oxygen species regulate autophagy through redox-sensitive proteases. Dev Cell 12: 484-485, 2007.
22. Xia P, Gou WF, Wang JJ, *et al*: Distinct radiosensitivity of lung carcinoma stem-like side population and main population cells. Cancer Biother Radiopharm 28: 471-478, 2013.
23. Xing YN, Deng P and Xu HM: Canstatin induces apoptosis in gastric cancer xenograft growth in mice through mitochondrial apoptotic pathway. Biosci Rep: Apr 2, 2014 (Epub ahead of print).
24. Phillips TM, McBride WH and Pajonk F: The response of $CD24^{-/low}/CD44^{+}$ breast cancer-initiating cells to radiation. J Natl Cancer Inst 98: 1777-1785, 2006.